Development 137, 169-176 (2010) doi:10.1242/dev.044867

Distinguishing direct from indirect roles for *bicoid* mRNA localization factors

Timothy T. Weil[1,2,3], Despina Xanthakis[1], Richard Parton[3], Ian Dobbie[3], Catherine Rabouille[1], Elizabeth R. Gavis[2,*] and Ilan Davis[3]

SUMMARY

Localization of *bicoid* mRNA to the anterior of the *Drosophila* oocyte is essential for patterning the anteroposterior body axis in the early embryo. *bicoid* mRNA localizes in a complex multistep process involving transacting factors, molecular motors and cytoskeletal components that remodel extensively during the lifetime of the mRNA. Genetic requirements for several localization factors, including Swallow and Staufen, are well established, but the precise roles of these factors and their relationship to *bicoid* mRNA transport particles remains unresolved. Here we use live cell imaging, super-resolution microscopy in fixed cells and immunoelectron microscopy on ultrathin frozen sections to study the distribution of Swallow, Staufen, actin and dynein relative to *bicoid* mRNA during late oogenesis. We show that Swallow and *bicoid* mRNA are transported independently and are not colocalized at their final destination. Furthermore, Swallow is not required for *bicoid* transport. Instead, Swallow localizes to the oocyte plasma membrane, in close proximity to actin filaments, and we present evidence that Swallow functions during the late phase of *bicoid* localization by regulating the actin cytoskeleton. In contrast, Staufen, dynein and *bicoid* mRNA form nonmembranous, electron dense particles at the oocyte anterior. Our results exclude a role for Swallow in linking *bicoid* mRNA to the dynein motor. Instead we propose a model for *bicoid* mRNA localization in which Swallow is transported independently by dynein and contributes indirectly to *bicoid* mRNA localization by organizing the cytoskeleton, whereas Staufen plays a direct role in dynein-dependent *bicoid* mRNA transport.

KEY WORDS: *Drosophila* oogenesis, *bicoid*, Intracellular mRNA localization, Swallow, Staufen, mRNA transport particles

INTRODUCTION

The asymmetric distribution of proteins within a cell is required to initiate and maintain cell polarity. In *Drosophila*, such protein asymmetries underlie axial polarity, assembly of germ plasm and neuronal development, and are often generated by translation of localized mRNAs (Jansen, 2001; Lopez de Heredia and Jansen, 2004; St Johnston, 2005). Translation of *bicoid* (*bcd*) mRNA that is localized at the anterior of the newly fertilized embryo results in a morphogenetic protein gradient that specifies anterior cell fates during subsequent development (Berleth et al., 1988; Driever et al., 1989; Driever and Nüsslein-Volhard, 1988a; Driever and Nüsslein-Volhard, 1988b; Driever and Nüsslein-Volhard, 1989). Localization of *bcd* is essential to produce the requisite concentrations of Bcd protein for embryonic patterning, as evidenced by the loss of anterior structures in mutants where *bcd* mRNA localization is disrupted.

Transcribed maternally in the ovarian nurse cells, *bcd* becomes localized during oogenesis via two temporally and genetically distinct pathways. During mid-oogenesis (stages 6-10a), transport of *bcd* to the anterior oocyte cortex requires microtubules, dynein, and the localization factor Exuperantia (Exu) (St Johnston, 2005). Exu is thought to associate with *bcd* in a ribonucleoprotein complex (RNP) in the nurse cells, and Exu function in the nurse cells is required to target the *bcd* RNP to the anterior cortex after it enters the oocyte (Cha et al., 2001; Wilhelm et al., 2000). However, the major phase of *bcd* localization occurs at late stages of oogenesis (from stage 10b onward), beginning with the onset of nurse cell dumping, when the nurse cells undergo apoptosis and extrude their cytoplasm into the oocyte (Weil et al., 2006). Using live imaging of fluorescently labeled *bcd* mRNA, we have previously shown that during this period, *bcd* accumulates at the anterior through continual transport on a specialized population of microtubules that are anchored to the actin cytoskeleton at the anterior cortex (Weil et al., 2006). The motility of *bcd* RNPs and their accumulation at the oocyte anterior during late stages of oogenesis requires dynein, suggesting that dynein is a component of the *bcd* transport RNP (Weil et al., 2006; Weil et al., 2008). However, colocalization of *bcd* and dynein has not been reported.

Anterior accumulation of *bcd* in late-stage oocytes also depends on the double-stranded RNA-binding protein Staufen (Stau) (St Johnston et al., 1989). Stau colocalizes with *bcd* mRNA at the anterior in late oocytes and early embryos (Weil et al., 2006; Weil et al., 2008), but it is not known whether Stau is a component of the *bcd* transport RNP or only becomes associated with *bcd* at the anterior cortex. In addition to Stau, Swallow (Swa), a 548 amino acid cytoplasmic protein with weak homology to a putative double-stranded-RNA-binding domain and a predicted coiled-coil domain (Chao et al., 1991; Lupas, 1996), functions selectively in the late-acting *bcd* localization pathway (St Johnston et al., 1989), most likely during the period of nurse cell dumping.

How Swa mediates *bcd* localization has been the subject of much debate. The biochemical isolation of Swa as a component of a *bcd* RNA-binding complex (Arn et al., 2003), the enrichment of Swa at the anterior cortex where *bcd* mRNA is localized (Schnorrer et al., 2000), and the mis-localization of both Swa and *bcd* to the posterior

[1]UMC Utrecht, Department of Cell Biology, Cell Microscopy Centre, AZU H02.313, Heildelberglaan 100, 3584 CX, Utrecht, The Netherlands. [2]Department of Molecular Biology, Princeton University, Princeton, NJ 08544, USA. [3]Department of Biochemistry, The University of Oxford, South Parks Road, Oxford, OX1 3QU, UK.

*Author for correspondence (gavis@princeton.edu)

Accepted 28 October 2009

of the oocyte in *gurken* (*grk*) mutants, in which oocyte microtubule polarity is altered (Schnorrer et al., 2000), have suggested that Swa may be transported together with *bcd* to the anterior cortex. Based on evidence that Swa interacts biochemically with Dynein light chain-1 in vitro and in vivo (Schnorrer et al., 2000), Swa has been proposed to act as an adaptor that links *bcd* to the dynein motor. In addition, Swa has been suggested to act by reorganizing a subset of oocyte microtubules through its interaction with the γ-tubulin ring complex (Schnorrer et al., 2002). Finally, the observations that endogenous Swa and Swa-GFP form relatively non-motile particles around the entire oocyte cortex and that *swa* mutants exhibit defects in microfilament organization have led to the proposition that Swa serves an anchoring function (Meng and Stephenson, 2002; Stephenson, 2004).

Here we use live cell imaging, super-resolution fluorescence microscopy and immunoelectron microscopy (IEM) on ultrathin frozen sections to investigate the relationship of Stau, Swa and dynein to *bcd* mRNA during the late phase of localization. We show that Swa and *bcd* mRNA do not reside in the same dynamic particle and do not colocalize at the anterior of the oocyte where *bcd* transcripts are maintained and anchored. Rather, Swa is localized to the plasma membrane, where it functions indirectly in *bcd* localization, probably by regulating the organization of the actin cytoskeleton that anchors anterior microtubules used for transport of *bcd* RNPs. Moreover, using a newly developed protocol for detection of mRNAs at the ultrastructural level, we show that *bcd* mRNA, Stau and dynein all colocalize in non-membrane-bound electron-dense particles near the anterior cortex, suggesting a direct role for these proteins in *bcd* mRNA transport. By distinguishing the roles of Swa and Stau in *bcd* localization, our results reveal diverse ways in which genetically identified localization factors contribute to mRNA transport.

MATERIALS AND METHODS

Fly strains

The following mutants and transgenic lines were used: *hsp83-MCP-GFP* (Forrest and Gavis, 2003), *hsp83-MCP-RFP* and *bcd-(ms2)$_6$* (Weil et al., 2006), *GFP-Stau* (Schuldt et al., 1998), *GFP-moe* (Edwards et al., 1997), *Swa-GFP* (Stephenson, 2004), *swa^{VA11}* and *swa^{TN62}* (gift of T. Schüpbach). *swa^{TN62}* produces a truncated Swa polypeptide and *swa^{VA11}* oocytes lack detectable Swa protein (Schnorrer et al., 2000). For analysis of the *swa* mutant phenotype, egg chambers homozygous for *swa^{TN62}* or trans-heterozygous for *swa^{VA11}* and *swa^{TN62}* were used, as homozygous *swa^{VA11}* females could not be obtained.

Preparation of oocytes for fluorescence imaging

For live fluorescence imaging, oocytes were prepared as described by Davis and Parton (Davis and Parton, 2005). Egg chambers from well-fed females were dissected and separated with tungsten needles in Series 95 halocarbon oil (KMZ Chemicals) on no. 1 coverslips (Corning).

For fixed tissue imaging, oocyte preparation followed Weil et al. (Weil et al., 2006). Ovaries from well-fed females were removed and fixed for 15 minutes in 4% electron microscopy grade paraformaldehyde (Polysciences) in PBS. Egg chambers were teased apart and washed several times with PBS before being mounted in either PBS or Vectashield (Vector Laboratories).

For drug treatments, oocytes were cultured and treated with cytochalasin D (Sigma) at a final concentration of 10 μg/ml, or colcemid (Sigma) final concentration 50 μg/ml, as previously described (Weil et al., 2006).

Fluorescence imaging

Single channel time-series imaging was performed with a wide-field DeltaVision microscope (Applied Precision, Olympus I×70 microscope, Roper Scientific CoolSNAP HQ camera) with a 100× oil objective. Images were deconvolved using Sedat/Agard algorithms with Applied Precision software. Confocal images of fixed material were collected with a Zeiss LSM 510 with 40× and 60× oil objectives.

Simultaneous multicolor live wide-field fluorescence microscopy was performed on OMX (Applied Precision). This microscope enables rapid collection of multicolor fluorescent image stacks using advanced control hardware/software and multiple cameras (Roper Scientific Cascade II) to simultaneously image multiple emission wavelengths. GFP and mRFP were excited at 488 nm and 594 nm through a 100×, 1.4 NA oil objective (Olympus). Fluorescence emissions were simultaneously collected onto two cameras to ensure temporal registration between the two fluorescence channels. Data was collected at three frames/second and deconvolved using Sedat/Agard algorithms with Applied Precision software.

Super-resolution imaging of fixed samples was done by 3D-Structured Illumination Microscopy (Schermelleh et al., 2008) using a 100×, 1.4NA oil objective (Olympus). The resultant images have resolutions of 145 nm in XY for GFP and 165 nm in XY for RFP channels.

Immunoelectron microscopy and in situ hybridization

For fixation of stage 13 oocytes for IEM, ovaries from well-fed females were isolated under Series 95 halocarbon oil (KMZ Chemicals) on a no. 1 coverslip (Corning). Using tungsten needles, stage 13 egg chambers were separated from ovarioles and aligned against a straight edge of a small piece of no. 1 coverslip submerged in 95 halocarbon oil. Sixteen per cent electron microscopy grade paraformaldehyde (Polysciences) was microinjected into the center of the oocyte using Femtotip needles (Eppendorf). Four per cent electron microscopy grade paraformaldehyde in PBS was then added to the oil around the injected egg chamber for 15 minutes. Following external fixation, tungsten needles were used to individually separate the egg chambers from the halocarbon oil and a glass Pasteur pipette (Fisherbrand) was used to remove the egg chamber from the coverslip and place it is an 1.5 ml Eppendorf tube. Fixed egg chambers were then stored in 1% electron microscopy grade paraformaldehyde in PBS until embedded.

In situ hybridization and IEM procedures followed standard protocol (Delanoue et al., 2007; Herpers and Rabouille, 2004). A hydrolyzed digoxigenin-labeled antisense *bcd* RNA probe was used, followed by sheep anti-digoxigenin (1:500; Roche Diagnostics) and rabbit anti-sheep antibody (1:750; Roche Diagnostics). For IEM the following antibodies were used: rabbit polyclonal anti-Dhc, Pep1 (1:300; gift of T. Hays); monoclonal anti-α-tubulin-FITC (1:5000; Sigma); rabbit polyclonal anti-GFP antibody (1:300; Abcam). Rabbit polyclonal antibodies were detected with protein A gold conjugates (Department of Cell Biology, Institute of Biomembranes, Utrecht, The Netherlands). Mouse antibodies were detected with rabbit anti-mouse antibody (1:250; Dako).

For each experiment, representative electron micrographs are displayed at optimal magnification. Microtubules were identified using morphological criteria based on previous studies (Delanoue et al., 2007; Herpers and Rabouille, 2004).

RESULTS

Swa is required for late-phase *bcd* mRNA localization

We have previously shown that the majority of *bcd* mRNA becomes localized at late stages of oogenesis, after the onset of nurse cell dumping [stages 10b-13 (Weil et al., 2006)]. Genetic analysis

Table 1. *bcd* mRNA localization in *swa* mutant oocytes at stage 11-13

Genotype	WT localization	No localization	Reduced localization	Mislocalization	Foci	Total
swa^{TN62}/swa^{VA11}	1 (2%)	28 (74%)	0 (0%)	6 (16%)	3 (8%)	38
swa^{TN62}/swa^{TN62}	4 (10%)	12 (29%)	6 (15%)	14 (34%)	5 (12%)	41
Wild type	52 (96%)	0 (0%)	0 (0%)	1 (2%)	1 (2%)	54

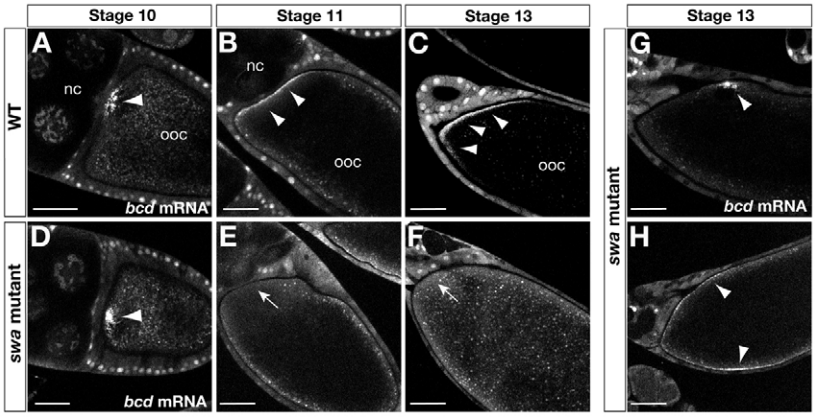

Fig. 1. Swa is required for *bcd* mRNA localization after stage 10. (**A-H**) Confocal images of wild-type (A-C) and *swa* mutant (D-H) egg chambers expressing *bcd*GFP*. Oocytes were fixed and GFP fluorescence was imaged directly. (A,D) Stage 10 egg chamber with *bcd*GFP* concentrated near the oocyte nucleus (arrowheads). (B,E) Stage 11 and (C,F) stage 13 egg chambers showing loss of anterior *bcd* localization in *swa* mutants (arrows verses arrowheads). (G,H) Additional *swa* mutant defects: (G) *bcd* concentrated near the oocyte nucleus (arrowhead) and (H) mis-localization of *bcd* along the lateral oocyte cortex (arrowheads). See Table 1 for quantitative analysis of the *swa* mutant phenotype. nc, nurse cells; ooc, oocyte. Scale bars: 20 μm in A,D; 50 μm in B,C,E-H.

indicates a requirement for *swa* in *bcd* mRNA localization beginning around the time of nurse cell dumping (Schnorrer et al., 2000; St Johnston et al., 1989). To investigate the specific function of Swa protein in the localization of *bcd* mRNA at late stages, when in situ hybridization is not reliable, we used the MS2 in vivo fluorescent tagging system to label endogenous *bcd* mRNA with GFP or RFP (designated as *bcd*GFP* or *bcd*RFP*, respectively). Fluorescently tagged *bcd* mRNA completely rescues the *bcd* mutant phenotype (Weil et al., 2006). We found that whereas wild-type and early-stage oocytes show no defects (Fig. 1A-D; Table 1), the majority of stage 11-13 *swa* mutant oocytes show loss of *bcd* mRNA localization (Fig. 1E-H; Table 1). We also detected two additional types of *bcd* mRNA localization defects that are reminiscent of defects previously detected by in situ hybridization to tissue sections (Pokrywka et al., 2000). In one type, foci of *bcd* mRNA are present near or along the anterior cortex and are commonly associated with the oocyte nucleus (Fig. 1G; Table 1). The second group shows mis-localized *bcd* mRNA along the lateral cortex of the oocyte (Fig. 1H; Table 1). These phenotypes are reminiscent of mRNA transport defects due to rearrangement or misorganization of the cytoskeleton, as reported for *bcd* mRNA in *grk* mutant oocytes (González-Reyes et al., 1995).

Swa does not play a direct role in *bcd* mRNA transport

Swa has been proposed to act as the link between *bcd* mRNA and the dynein motor (Schnorrer et al., 2000). Such a direct role for Swa in *bcd* mRNA transport predicts that Swa should be detectable within transport particles traveling together with *bcd* mRNA and possibly with the mRNA at its final destination. We first tested whether Swa is intimately associated with the *bcd* mRNA transport particle. Using conventional sequential imaging on a wide-field DeltaVision microscope we established that both Swa and *bcd* RNA are transported in particles towards the anterior (data not shown) (Weil et al., 2008). However, the relatively slow speed of sequential imaging, at less than one frame in two channels per second, did not allow us to conclusively determine

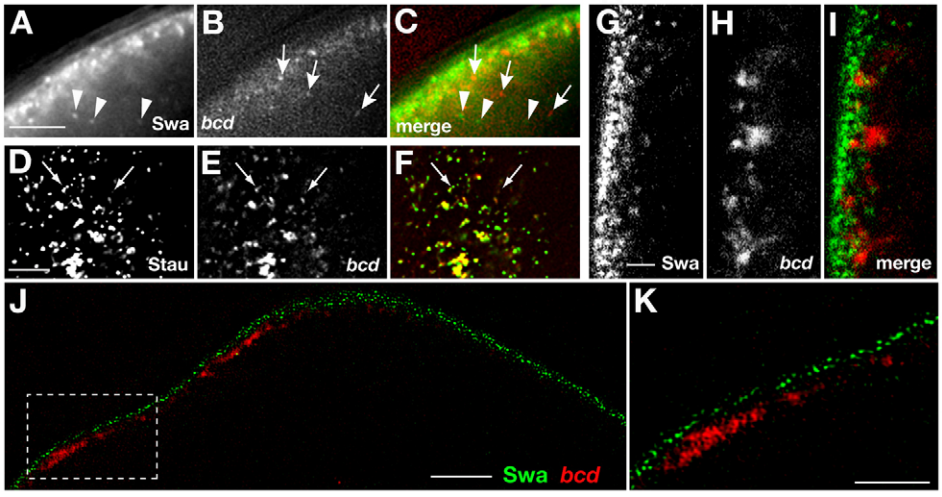

Fig. 2. *bcd* mRNA and Swa move independently and do not colocalize at the anterior cortex. (**A-C**) Anterior region of a stage 12/13 oocyte. Images of Swa-GFP (A) and *bcd*RFP* (B) were acquired simultaneously on the OMX. Individual particles determined to be dynamic over 20 frames (6.5 seconds) are indicated by arrows and arrowheads. The single frame image (C) shows that Swa-GFP and *bcd*RFP* particles are independent. (**D-F**) Anterior region of a stage 12 oocyte. Images of GFP-Stau (D) and *bcd*RFP* (E) were acquired simultaneously on the OMX. The majority of *bcd*RFP* colocalize with Stau-GFP (F), whereas some Stau particles lack *bcd* mRNA, consistent with previous results (Weil et al., 2006). Colocalized particles are observed undergoing directed runs (arrows). (**G-I**) Confocal images of stage 12/13 egg chambers expressing Swa-GFP and *bcd*RFP*. Swa-GFP (G) and *bcd*RFP* (H) show minimal overlap at the oocyte anterior cortex (I). (**J**,**K**) Swa-GFP and *bcd*RFP* detected using the OMX structured illumination mode. At this resolution, Swa and *bcd* are entirely separable. (K) Magnification of the boxed region in J. Scale bars: 5 μm in A-F; 4 μm in J; 2 μm in G-I,K.

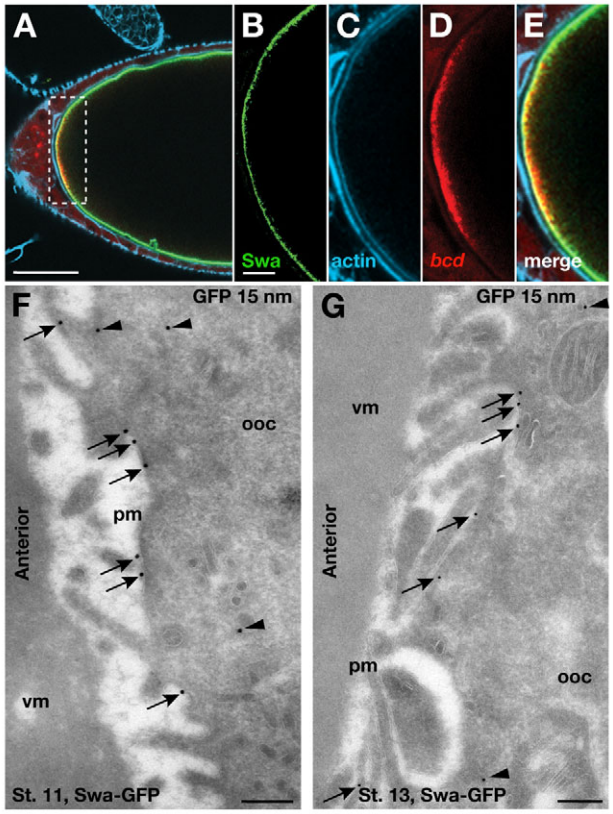

Fig. 3. Swa is localized to the plasma membrane. (**A**) Confocal image of a fixed stage 13 egg chamber expressing Swa-GFP and *bcd*RFP*. Actin is stained with far-red phalloidin. (**B-E**) Magnification of the boxed region in A. Swa protein (B) and actin (C) appear to overlap at the anterior cortex, whereas the majority of *bcd* mRNA (D) resides outside this region (E). (**F**,**G**) IEM localization of Swa-GFP at the anterior cortex of stage 11 (F) and stage 13 (G) egg chambers expressing Swa-GFP, using anti-GFP antibody (15 nm). The majority of Swa is detected on the plasma membrane (arrows), with a small cytoplasmic population (arrowheads), consistent with fluorescence images (Fig. 2A). Note that Swa is detected at the plasma membrane along the entire cortex (not shown). pm, plasma membrane; ooc, oocyte; vm, vitelline membrane. Scale bars: 50 μm in A; 10 μm in B-E; 200 nm in F,G.

whether Swa and *bcd* mRNA are co-transported in the same particle. To address this issue, we utilized the simultaneous acquisition function of a replica of the OMX (Optical Microscope Experimental) system, a prototype wide-field instrument developed by Prof. John Sedat and colleagues at University of California, San Francisco (Schermelleh et al., 2008). The complete redesign of the light path and the use of laser illumination by the OMX enabled us to collect rapid time-lapse series from a single excitation event in multiple emission channels simultaneously. Examining stage 12 oocytes co-expressing Swa-GFP and *bcd*RFP* with this microscope showed conclusively that Swa particles move independently of *bcd*RFP* particles at the anterior cortex (Fig. 2A-C). As previously described (Weil et al., 2008), a high percentage of *bcd* mRNA particles show movement and particles display long direct runs laterally and toward the anterior. Conversely, particles of Swa show a lower amount of overall movement at the oocyte cortex. Upon careful examination, we detected occasional directed runs of Swa particles indicative of active transport (see Movie 1 in the supplementary material), consistent with previous biochemical data connecting Swa to dynein (Schnorrer et al., 2000). We conclude that Swa cannot be acting as a link connecting *bcd* mRNA to dynein during anterior transport. However, this does not exclude the possibility that Swa could act after *bcd* arrives the anterior cortex, possibly as a transient tether.

To determine if Swa acts as a transient anchor for *bcd* mRNA following anterior transport, we tested whether or not Swa protein and *bcd* mRNA colocalize at the anterior cortex. Using conventional confocal microscopy, we found that *bcd* mRNA and Swa protein are in the same region of cytoplasm. However, close inspection suggested that the protein and mRNA localizations are inter-digitated with only some regions of overlap (Fig. 2G-I). To address this question with greater resolution we used the super-resolution mode of acquisition of the OMX system, which provides approximately twofold greater resolution than conventional light microscopy (see Materials and methods). By this method, we detected no overlap of Swa protein and *bcd* mRNA at the anterior cortex (Fig. 2J,K). Specifically, discrete particles of Swa protein are tightly apposed to the entire cortex, including the anterior, whereas particles of *bcd* reside at a greater distance from the cortex and are present only at the anterior. From these data, we conclude that Swa is not directly associated with *bcd* mRNA at any point during the late phase of localization. Therefore, Swa cannot be acting as the link between dynein and *bcd* mRNA, either during its transport or to maintain its localization at the final destination.

Swa is localized to the plasma membrane in late oocytes in close proximity to actin filaments

Swa and *bcd* mRNA are transported and localized independently of each other, yet Swa is required for *bcd* mRNA localization. To resolve this apparent contradiction, we first examined the specific subcellular distribution of Swa. Given that Swa is localized at the cortex, where the actin cytoskeleton is enriched, we first imaged late-stage oocytes expressing Swa-GFP and *bcd*RFP*, stained with phalloidin (Fig. 3A-E). As expected, *bcd* mRNA shows minimal overlap with Swa. Conversely, we found that Swa and actin are tightly apposed at the cortex, although it was difficult to determine convincingly whether they colocalize using light microscopy.

Therefore, to resolve the localization of Swa, we used IEM on ultrathin frozen sections of late-stage oocytes (see Materials and methods). We examined sections of oocytes expressing Swa-GFP at stage 11, when *bcd* mRNA is maintained at the anterior by continual active transport (Weil et al., 2006), labeled using an anti-GFP antibody and gold conjugates. We found that 72% of the gold particles (n=288) are localized to the oocyte plasma membrane (Fig. 3F, arrows). We also detected a small pool of cytoplasmic Swa (Fig. 3F, arrowheads). As wild-type stage 11-13 oocytes stained with anti-GFP antibody do not show any labeling at the anterior (see Fig. S1 in the supplementary material), we conclude that the cytoplasmic labeling of Swa-GFP is specific and could correspond to the pool of Swa in transit, as suggested by results from fluorescence experiments (see Movie 1 in the supplementary material).

To examine the distribution of Swa at the end of oogenesis, when *bcd* mRNA transitions to a static anchor (Weil et al., 2008), we had to develop new methods. Conventional fixation methods are not effective because of the deposition of vitelline membrane and chorion, but fixation can be accomplished through direct injection of fixative (see Materials and methods). This method then allowed

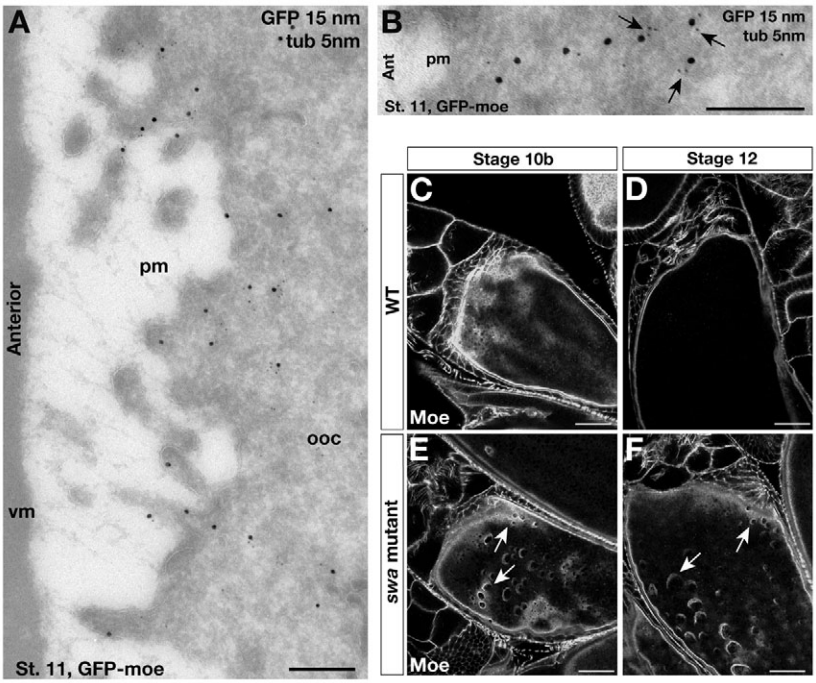

Fig. 4. Cortical actin is localized near the plasma membrane and organized by Swa. (**A**,**B**) IEM localization of GFP-moe at the anterior cortex of stage 11 egg chambers expressing GFP-moe and labeled with anti-GFP (15 nm) and anti-tubulin (5 nm) antibodies. (A) GFP-moe is detected near, but not on, the plasma membrane. (B) High magnification image of a GFP-moe labeled 'filament', showing its association with microtubules (arrows). (**C-F**) Direct fluorescence confocal images of fixed wild-type (C,D) and *swa* mutant (E,F) egg chambers expressing GFP-moe. Cortical actin organization is disrupted in stage 10b (E) and stage 12 (F) oocytes compared with the wild type (C,D). Holes in the cortex are observed at the anterior (arrows) and throughout the oocyte. pm, plasma membrane; ooc, oocyte; vm, vitelline membrane. Scale bars: 200 nm in A,B; 20 μm in C-F.

us to carry out standard sectioning of frozen sections and immunolabeling. Using this technique, we showed that Swa remains associated with the plasma membrane at stage 13 (Fig. 3G, arrows).

To visualize cortical actin, we immunolabeled egg chambers expressing a GFP fusion to the actin-binding protein moesin (GFP-moe) with anti-GFP antibody. We found that GFP-moe localizes near the oocyte plasma membrane and appears to extend away from the cortex in profiles consistent with filaments (Fig. 4A,B), which are often associated with microtubules (Fig. 4B, arrows). Together, these results suggest that Swa and cortical actin occupy distinct subcellular locations but are in very close proximity to each other, consistent with a role for Swa in the organization of the cytoskeleton.

Swa is required to organize the actin cytoskeleton in late oogenesis

Our previous work has shown that actin functions to maintain anterior microtubules required for the continual active transport of *bcd* mRNA from stage 10b to 13 (Weil et al., 2006). Foci of *bcd* mRNA that we observed in *swa* mutant oocytes (Fig. 1G) are very reminiscent of *bcd* aggregates that form upon disruption of the actin cytoskeleton (data not shown) (Weil et al., 2006). This similarity, together with their proximity at the plasma membrane suggests a link between Swa and the actin cytoskeleton in localization of *bcd* mRNA. To test this hypothesis we first treated late-stage oocytes expressing Swa-GFP with cytochalasin D to disrupt actin filaments. In these oocytes, the majority of Swa protein remains cortically localized (data not shown). These results indicate that actin is unlikely to be required for the localization or maintenance of Swa at the cortex. By contrast, examination of stage 10b-14 *swa* mutant oocytes expressing the GFP-moe revealed large imperfections and holes in the cortical actin cytoskeleton (Fig. 4C-F), indicating that actin organization is severely compromised compared with wild-type oocytes. These results are consistent with a previous study that visualized actin by phalloidin staining of fixed specimens (Meng and Stephenson, 2002). Thus, we conclude that Swa is required for proper actin organization in the late stages of oogenesis.

We interpret our results as suggesting that *bcd* mRNA localization defects observed in *swa* mutant oocytes are due to disruption of the actin cytoskeleton, resulting, in turn, in failure to anchor the anterior microtubules to the cortex. Visualization of *bcd*GFP* at high temporal and spatial resolution showed that *bcd* mRNA particles that form foci in *swa* mutant oocytes are highly dynamic, and appear to undergo more frequent directed runs than in wild-type oocytes (see Movies 2 and 3 in the supplementary material). Moreover, similarly to wild-type oocytes, movement of *bcd* particles in *swa* mutant oocytes ceases upon microtubule depolymerization (data not shown). Together, these results suggest that in the absence of Swa, *bcd* mRNA particles continue to move on microtubules, but the minus ends of these microtubules are no longer anchored to the anterior cortex (see Movie 2 in the supplementary material). We conclude that Swa functions indirectly in late-phase *bcd* mRNA localization by regulating or organizing the actin cytoskeleton, which in turn anchors the anterior microtubules.

bcd mRNA, Stau and dynein localize to electron-dense particles at the anterior of late-stage oocytes

In addition to Swa, we have previously shown that both Stau and dynein are required for the localization of *bcd* mRNA at the oocyte anterior during late-phase localization (Weil et al., 2006). Stau also plays a role in cortical anchoring of *bcd* during the transition from oogenesis to embryogenesis (St Johnston et al., 1989). Stau and *bcd* localize at the anterior oocyte cortex coincidently and colocalize in particles at the anterior in both the oocyte and early embryo (Weil et al., 2008). However, previous studies have not resolved whether Stau is an integral component of the *bcd* transport RNP or whether, like Swa, Stau is transported to the anterior independently of *bcd* and participates in maintaining *bcd* after its arrival at the cortex. Additionally, hypomorphic Dynein heavy chain (Dhc) mutations eliminate *bcd* mRNA particle motility and greatly reduce anterior accumulation (Weil et al., 2008), suggesting that dynein is also a component of the *bcd* RNP, but no association with Stau has been reported.

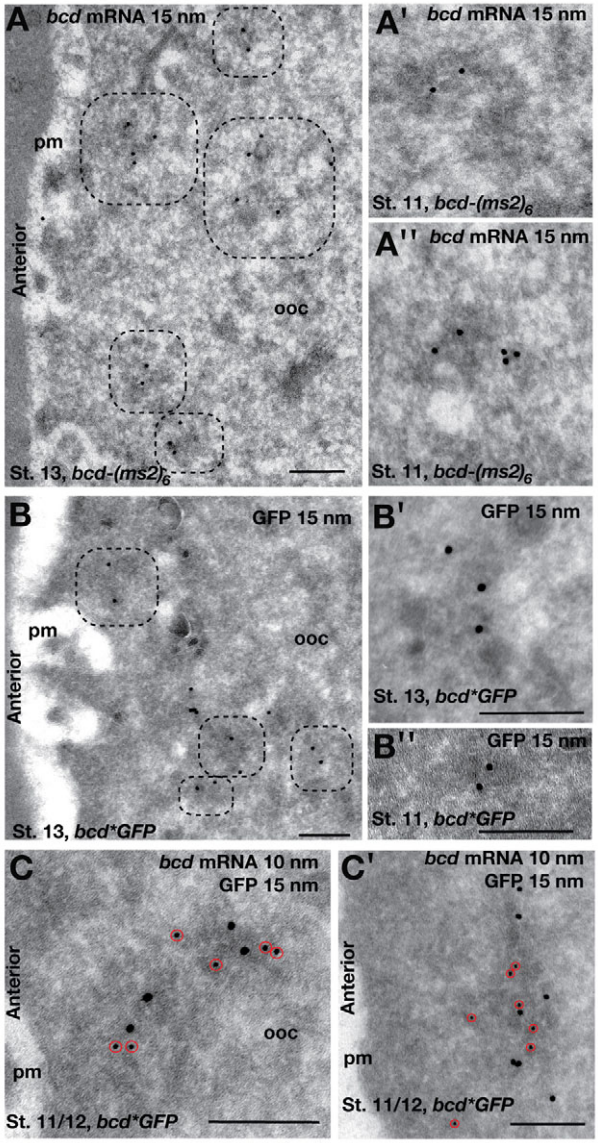

Fig. 5. *bcd* mRNA is present in electron-dense particles near the anterior cortex. (**A-A″**) ISH-IEM localization of *bcd* mRNA in ultrathin frozen sections of stage 13 (A) and stage 11 (A′,A″) egg chambers expressing four copies of *bcd*-$(ms2)_6$ using a digoxigenin-labeled antisense *bcd* riboprobe and anti-digoxigenin antibody (15 nm). (A) *bcd* mRNA is present in electron-dense particles at the anterior oocyte cortex (dashed black boxes). (A′,A″) High magnification images from additional samples. (**B**) IEM localization of *bcd*GFP* in a stage 13 egg chamber expressing *bcd*GFP*, using anti-GFP antibody (15 nm), shows its presence in electron-dense particles near the anterior oocyte cortex. (**B′**,**B″**) High magnification images from additional samples at the indicated stages. (**C**,**C′**) Double labeling of *bcd*GFP* detected by ISH-IEM using a digoxigenin-labeled anti-sense *bcd* riboprobe and anti-digoxigenin antibody (10 nm, red circle) and IEM using anti-GFP antibody (15 nm) in stage 11/12 oocytes expressing *bcd*GFP*. Note that both are detected in the same dense particles. ooc, oocyte; pm, plasma membrane. Scale bars: 200 nm.

Using the simultaneous acquisition function of the OMX to image stage 12 egg chambers expressing GFP-Stau and *bcd*RFP*, we observed colocalization of *bcd* and Stau in motile particles (Fig. 2D-F). We then further characterized *bcd* particles at the ultrastructural level by co-visualizing *bcd* mRNA with Stau and Dhc. These experiments used a protocol that was recently developed to perform RNA in situ hybridization followed by IEM (ISH-IEM) on ultrathin frozen sections. The use of oocytes from females expressing four copies of the *bcd*-$(ms2)_6$ transgene, which produces MS2-tagged *bcd* mRNA in addition to wild-type *bcd* mRNA, maximized detection by the *bcd* probe. ISH-IEM of *bcd* mRNA showed that *bcd* is present in electron-dense particles near the anterior cortex that are neither bound to the membrane nor associated with vesicles (Fig. 5A-A″; see Fig. S1B in the supplementary material). *bcd* mRNA particles show an average area of 0.04 μm^2 and a gold density of 82.9 g/μm^2 (n=30) but appear less dense and less compact than *grk* mRNA particles (Delanoue et al., 2007). By contrast, the surrounding cytoplasm show a much lower gold density of 1.2 g/μm^2 (n=18). When *bcd*-$(ms2)_6$ mRNA is bound by MCP-GFP, we were able to detect *bcd*GFP* with an anti-GFP antibody. The labeling was also found in dense particles, similar to the ones described above (Fig. 5B-B″). This was confirmed by double-labeling experiments in which *bcd* mRNA was detected by both ISH-IEM and by anti-GFP immunolabeling (Fig. 5C,C′). By contrast, the free MCP-GFP was not detected (see Fig. S1C in the supplementary material).

To determine whether Stau is also associated with these dense particles, we labeled sections of stage 11/12 oocyte expressing GFP-Stau with an anti-GFP antibody. Similarly to *bcd* mRNA, Stau is localized to non-membrane-bound dense particles (Fig. 6A,A′). Co-visualization of Stau-GFP and *bcd* mRNA confirmed that they are present in the same dense particles (Fig. 6B). These particles are specific to the anterior oocyte region, as the lateral regions of the same immunolabeled sections do not show specific labeling (see Fig. S2A-D in the supplementary material).

We next tested whether the observed *bcd*/Stau particles contain dynein by co-immunodetection of Dhc with either *bcd*GFP* or GFP-Stau using anti-Dhc and anti-GFP antibodies, respectively. We found that Dhc is present in the same particles as *bcd* mRNA (Fig. 6C) or Stau (Fig. 6D,E). As our previous work showed that *bcd* mRNA moves directly on microtubules (Weil et al., 2008), we then aimed to visualize the cellular distribution of microtubules in relation to the electron-dense particles. Microtubule arrays in stage 11 nurse cells are readily visible by IEM with an anti-tubulin antibody, but we detected the anterior population of oocyte microtubules much less frequently (see Fig. S3 in the supplementary material). We interpret these results as indicating that at late stages the oocyte anterior microtubules are either few in number or structurally modified so that they are not detected by the antibody, or that they are highly dynamic and thus not preserved during fixation. Nonetheless, in some sections, unlabeled microtubules are visible near the anterior cortex, and occasionally we detected adjacent particles (Fig. 6E). Taken together, these data indicate that *bcd* mRNA is present in electron-dense particles that contain Stau and dynein. Based on the functional requirement for dynein in *bcd* mRNA transport (Weil et al., 2008), we propose that the *bcd* mRNA particles we observe are being transported to the anterior by dynein.

DISCUSSION

Anterior localization of *bcd* mRNA during oogenesis is essential for anteroposterior axis specification in the early embryo. A number of factors, including Exu, Stau and Swa are required for *bcd* mRNA localization, but whether they participate directly or indirectly in *bcd* transport and/or anchoring has remained unclear. Here, we show that Swa is not a component of *bcd* transport RNPs, nor does it colocalize with *bcd* at the anterior oocyte cortex. We provide data supporting a model in which Swa acts

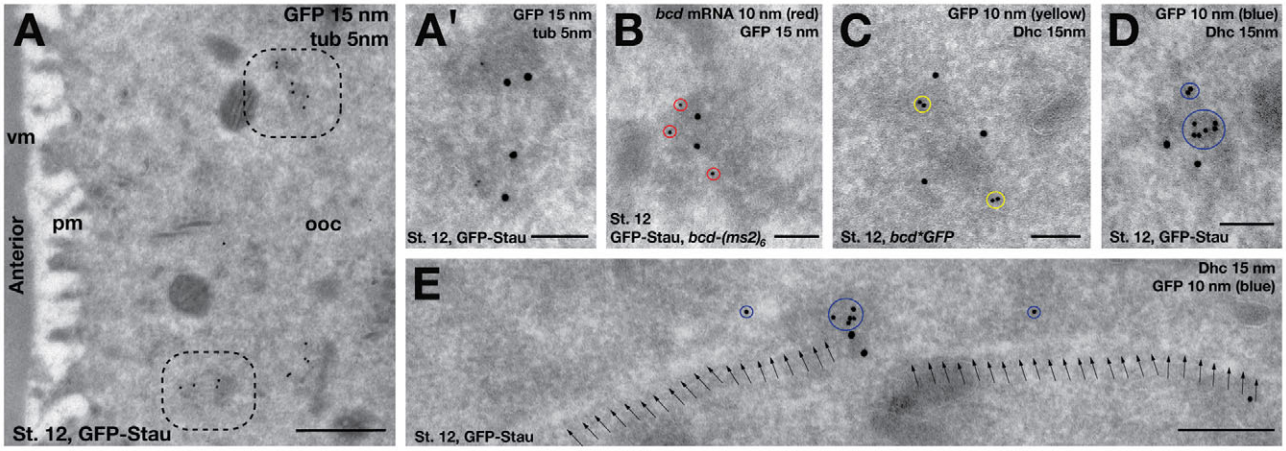

Fig. 6. Stau, *bcd* mRNA and Dhc are in the same transport particle. (A,A′,B,D,E) IEM images of the anterior region of stage 12 egg chambers expressing GFP-Stau. (**A**) Anti-GFP (15 nm) and anti-tubulin (5 nm) staining shows GFP-Stau in electron-dense particles at a short distance from the anterior cortex (dashed black boxes). (**A′**) Higher magnification of a particle. (**B**) ISH-IEM for *bcd* mRNA (10 nm, red circle) followed by anti-GFP detection of GFP-Stau (15 nm) shows that *bcd* and Stau are in the same dense particle. (**C**) *bcd*GFP* (10 nm, yellow circle) followed by anti-Dhc (15 nm) labeling shows *bcd*GFP* in particles together with dynein motor components. (**D**,**E**) GFP-Stau and Dhc are detected in the same particle. (D) GFP-Stau (10 nm, blue circle) and Dhc second (15 nm) or (E) Dhc is labeled first (15 nm) and GFP-Stau second (10 nm, blue circle). These particles, which we propose to be transport particles, can be detected adjacent to microtubules (arrows). ooc, oocyte; pm, plasma membrane; vm, vitelline membrane. Scale bars: 500 nm in A; 100 nm in A′,B,C,D; 200 nm in E.

indirectly, by regulating the organization of the cortical actin cytoskeleton, which in turn maintains the specialized anterior population of microtubules essential for the late phase of *bcd* RNP transport. By contrast, dynein and Stau are closely associated with *bcd* mRNA in nonmembranous electron-dense particles, consistent with a direct role for Stau in dynein-dependent transport of *bcd* mRNA to the anterior (Fig. 7).

A direct role for Swa in either transport or anchoring of *bcd* mRNA predicts and requires that the protein be colocalized with *bcd* mRNA during transport or anchoring. Here we have tested this prediction conclusively in three ways. First, we used an OMX microscope with highly sensitive and rapid multi-channel imaging to study to movement of Swa and *bcd* RNA particles simultaneously. Second, we took advantage of the increased resolution of the OMX microscope with fixed material to analyze the precise locations of Swa and *bcd* at the anterior oocyte cortex. Importantly, our results show conclusively that Swa and *bcd* mRNA move independently to the anterior and occupy distinct domains at the anterior cortex. Third, we determined the subcellular distributions of Swa and *bcd* at EM resolution, demonstrating that *bcd* is mostly in particles near the anterior cortex (see below) whereas Swa is mostly confined to the plasma membrane of the entire oocyte. How the membrane association of Swa, which does not contain a transmembrane domain and is not predicted to harbor lipid modifications, is mediated remains to be investigated.

At the plasma membrane, Swa is found in close proximity to the cortical actin cytoskeleton. Together with the defects in the cortical actin cytoskeleton observed in *swa* mutants, this indicates a role for Swa in organization of the actin cytoskeleton. Whereas the actin cytoskeleton is not required for anchoring *bcd* at the anterior cortex until the very end of oogenesis (Weil et al., 2008), it plays an indirect role in *bcd* localization by anchoring the anterior microtubules required for the continual transport of *bcd* during stages 11-13. Our results indicate that, in *swa* mutants, these microtubules remain intact but are not properly attached to or organized at the cortex, such that *bcd* transport is non-productive.

Swa is not limited to the anterior, however, and can be detected along the entire cortex of the oocyte. Moreover, in *swa* mutants, the cortical actin cytoskeleton is disrupted throughout the entire oocyte. Accordingly, some *swa* alleles show defects in posterior localization of *osk* mRNA at late stages of oogenesis (Pokrywka et al., 2004) (S. Bergsten and E.R.G., unpublished). As actin is required for *osk* mRNA anchoring, this phenotype could be a result of disruption of the actin cytoskeleton. Clues as to how Swa regulates the actin cytoskeleton are not readily apparent from the Swa protein sequence, and an understanding of this mechanism awaits further biochemical analysis of Swa.

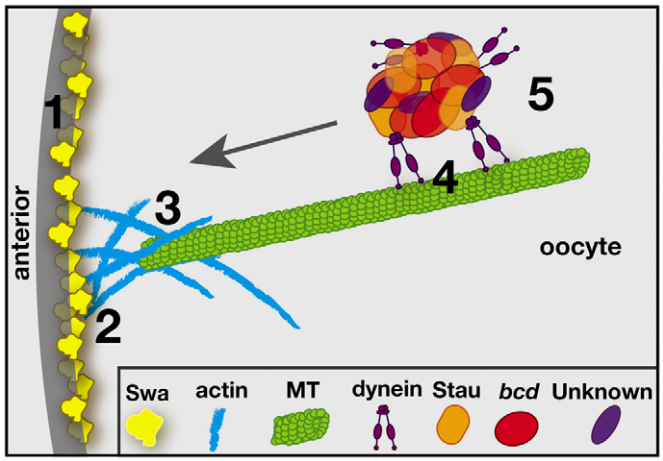

Fig. 7. Model for *bcd* mRNA localization in late oogenesis. In late-stage oocytes, Swa protein is localized and maintained at the plasma membrane around the entire oocyte (1). Swa protein functions in the organization of the actin cytoskeleton (2), which in turn acts to anchor an anterior population of microtubules (3) required for the continual active transport of *bcd* mRNA (4). The nonmembranous *bcd* RNP contains *bcd* mRNA, Stau and dynein motor complex components and additional factors not illustrated here (5).

Our IEM results provide direct evidence that *bcd* mRNA is packaged with Stau and dynein into RNPs that are enriched at, and presumably transported to, the anterior after stage 10b. Indeed, live imaging using the OMX system showed co-transport of *bcd* and Stau in the same dynamic particles. In addition to its role in *bcd* localization, Stau is a key component of *osk* RNPs and is required for kinesin-dependent transport of *osk* to the oocyte posterior. Thus, Stau is a component of two independent transport RNPs, each associated with a different motor protein for transport to distinct locations within the oocyte. Whether Stau, which contains five double-stranded RNA-binding domains, interacts directly with *bcd* and *osk* mRNAs or indirectly by association with sequence-specific mRNA-binding proteins, remains to be determined. However, structure/function analysis of Stau suggests that different Stau double-stranded RNA-binding domains may determine which transport factors are linked to each mRNA (Micklem et al., 2000; Ramos et al., 2000). Furthermore, as Stau functions in *osk* localization during stages 8-9 but is required for *bcd* localization only after stage 10b, the assembly of Stau/*bcd* transport complexes must be temporally regulated. Stau is also required during the oocyte-to-embryo transition, for the redistribution of *bcd* from its tight cortical distribution in the oocyte to its more diffuse anterior distribution in the early embryo (St Johnston et al., 1989). We have previously shown that Stau colocalizes with *bcd* mRNA when it is anchored to the actin cytoskeleton at the latest stages of oogenesis and is retained by *bcd* particles in the early embryo (Weil et al., 2008). Thus, Stau remains an integral component of *bcd* RNPs as they are remodeled from transport to anchoring complexes and finally to their translationally active state in the embryo. In the future, detailed biochemical analysis combined with advanced imaging methods that permit detection of in vivo RNA-protein and protein-protein interactions will be necessary to ascertain how specificity is conferred on localization and anchoring.

Acknowledgements

We are grateful to T. Schüpbach, E. Stephenson, D. Kiehart, T. Hays and D. St Johnston for fly stocks and antibodies, J. Goodhouse for assistance with confocal microscopy and all members of the Cell Microscopy Center in Utrecht, NL for assistance with electron microscopy. The analysis of Swa was initiated by K. Forrest (Princeton) and benefitted from his intellectual contributions. This work was supported by a Marie Curie International Incoming Fellowship (ROXA0) to T.T.W., grant from the National Institutes of Health (GM067758) to E.R.G. and Wellcome Trust Senior Research Fellowship (081858) to I.D. Deposited in PMC for release after 6 months.

Supplementary material

Supplementary material for this article is available at
http://dev.biologists.org/lookup/suppl/doi:10.1242/dev.044867/-/DC1

References

Arn, E. A., Cha, B. J., Theurkauf, W. E. and Macdonald, P. M. (2003). Recognition of a *bicoid* mRNA localization signal by a protein complex containing Swallow, Nod, and RNA binding proteins. *Dev. Cell* **4**, 41-51.

Berleth, T., Burri, M., Thoma, G., Bopp, D., Richstein, S., Frigerio, G., Noll, M. and Nüsslein-Volhard, C. (1988). The role of localization of *bicoid* RNA in organizing the anterior pattern of the *Drosophila* embryo. *EMBO J.* **7**, 1749-1756.

Cha, B. J., Koppetsch, B. S. and Theurkauf, W. E. (2001). In vivo analysis of *Drosophila bicoid* mRNA localization reveals a novel microtubule-dependent axis specification pathway. *Cell* **106**, 35-46.

Chao, Y. C., Donahue, K. M., Pokrywa, N. J. and Stephenson, E. C. (1991). Sequence of *swallow*, a gene required for the localization of *bicoid* message in *Drosophila* eggs. *Dev. Genet.* **12**, 333-341.

Davis, I. and Parton, R. (2005). Time-lapse cinematography in living *Drosophila* tissue. In *Live Cell Imaging: A Laboratory Manual* (ed. S. A. Goldman), pp. 385-407. Cold Spring Harbor, NY: Cold Spring Harbor Laboratory Press.

Delanoue, R., Herpers, B., Soetaert, J., Davis, I. and Rabouille, C. (2007). *Drosophila* Squid/hnRNP helps Dynein switch from a *gurken* mRNA transport motor to an ultrastructural static anchor in sponge bodies. *Dev. Cell* **13**, 523-538.

Driever, W. and Nüsslein-Volhard, C. (1988a). A gradient of bicoid protein in *Drosophila* embryos. *Cell* **54**, 83-93.

Driever, W. and Nüsslein-Volhard, C. (1988b). The bicoid protein determines position in the *Drosophila* embryo in a concentration-dependent manner. *Cell* **54**, 95-104.

Driever, W. and Nüsslein-Volhard, C. (1989). The bicoid protein is a positive regulator of *hunchback* transcription in the early *Drosophila* embryo. *Nature* **337**, 138-143.

Driever, W., Ma, J., Nüsslein-Volhard, C. and Ptashne, M. (1989). Rescue of *bicoid* mutant *Drosophila* embryos by bicoid fusion proteins containing heterologous activating sequences. *Nature* **342**, 149-153.

Edwards, K. A., Demsky, M., Montague, R. A., Weymouth, N. and Kiehart, D. P. (1997). GFP-moesin illuminates actin cytoskeleton dynamics in living tissue and demonstrates cell shape changes during morphogenesis in *Drosophila*. *Dev. Biol.* **191**, 103-117.

Forrest, K. M. and Gavis, E. R. (2003). Live imaging of endogenous mRNA reveals a diffusion and entrapment mechanism for *nanos* mRNA localization in *Drosophila*. *Curr. Biol.* **13**, 1159-1168.

González-Reyes, A., Elliot, H. and St Johnston, D. (1995). Polarization of both major body axes in *Drosophila* by *gurken-torpedo* signalling. *Nature* **375**, 654-658.

Herpers, B. and Rabouille, C. (2004). mRNA localization and ER-based protein sorting mechanisms dictate the use of transitional endoplasmic reticulum-golgi units involved in *gurken* transport in *Drosophila* oocytes. *Mol. Biol. Cell* **15**, 5306-5317.

Jansen, R.-P. (2001). mRNA localization: message on the move. *Nat. Rev. Mol. Cell Biol.* **2**, 247-256.

Lopez de Heredia, M. and Jansen, R. P. (2004). mRNA localization and the cytoskeleton. *Curr. Opin. Cell Biol.* **16**, 80-85.

Lupas, A. (1996). Prediction and analysis of coiled-coil structures. *Methods Enzymol.* **266**, 513-525.

Meng, J. and Stephenson, E. C. (2002). Oocyte and embryonic cytoskeletal defects caused by mutations in the *Drosophila swallow* gene. *Dev. Genes Evol.* **212**, 239-247.

Micklem, D. R., Adams, J., Grunert, S. and St Johnston, D. (2000). Distinct roles of two conserved Staufen domains in *oskar* mRNA localization and translation. *EMBO J.* **19**, 1366-1377.

Pokrywka, N. J., Fishbein, L. and Frederick, J. (2000). New phenotypes associated with the *swallow* gene of *Drosophila*: evidence for a general role in oocyte cytoskeletal organization. *Dev. Genes Evol.* **210**, 426-435.

Pokrywka, N. J., Meng, L., Debiec, K. and Stephenson, E. C. (2004). Identification of hypomorphic and null alleles of *swallow* via molecular and phenotypic analyses. *Dev. Genes Evol.* **214**, 185-192.

Ramos, A., Grunert, S., Adams, J., Micklem, D. R., Proctor, M. R., Freund, S., Bycroft, M., St Johnston, D. and Varani, G. (2000). RNA recognition by a Staufen double-stranded RNA-binding domain. *EMBO J.* **19**, 997-1009.

Schermelleh, L., Carlton, P. M., Haase, S., Shao, L., Winoto, L., Kner, P., Burke, B., Cardoso, M. C., Agard, D. A., Gustafsson, M. G. et al. (2008). Subdiffraction multicolor imaging of the nuclear periphery with 3D structured illumination microscopy. *Science* **320**, 1332-1336.

Schnorrer, F., Bohmann, K. and Nüsslein-Volhard, C. (2000). The molecular motor dynein is involved in targeting *swallow* and *bicoid* RNA to the anterior pole of *Drosophila* oocytes. *Nat. Cell Biol.* **2**, 185-190.

Schnorrer, F., Luschnig, S., Koch, I. and Nüsslein-Volhard, C. (2002). γ-*Tubulin37C* and γ-*tubulin ring complex protein 75* are essential for *bicoid* RNA localization during *Drosophila* oogenesis. *Dev. Cell* **3**, 685-696.

Schuldt, A. J., Adams, J. H., Davidson, C. M., Micklem, D. R., Haseloff, J., St Johnston, D. and Brand, A. H. (1998). Miranda mediates asymmetric protein and RNA localization in the developing nervous system. *Genes Dev.* **12**, 1847-1857.

St Johnston, D. (2005). Moving messages: the intracellular localization of mRNAs. *Nat. Rev. Mol. Cell Biol.* **6**, 363-375.

St Johnston, D., Driever, W., Berleth, T., Richstein, S. and Nüsslein-Volhard, C. (1989). Multiple steps in the localization of *bicoid* RNA to the anterior pole of the *Drosophila* oocyte. *Development* **107 Suppl.**, 13-19.

Stephenson, E. C. (2004). Localization of Swallow-Green fluorescent protein in *Drosophila* oogenesis and implications for the role of Swallow in RNA localization. *Genesis* **39**, 280-287.

Weil, T. T., Forrest, K. M. and Gavis, E. R. (2006). Localization of *bicoid* mRNA in late oocytes is maintained by continual active transport. *Dev. Cell* **11**, 251-262.

Weil, T. T., Parton, R., Davis, I. and Gavis, E. R. (2008). Changes in *bicoid* mRNA anchoring highlight conserved mechanisms during the oocyte-to-embryo transition. *Curr. Biol.* **18**, 1055-1061.

Wilhelm, J. E., Mansfield, J., Hom-Booher, N., Wang, S., Turck, C. W., Hazelrigg, T. and Vale, R. D. (2000). Isolation of a ribonucleoprotein complex involved in mRNA localization in *Drosophila* oocytes. *J. Cell Biol.* **148**, 427-440.